LOAD TRANSFER AND STRESS IN A PILED GRAVITY RETAINING WALL

QUN CHEN, LI WAN, CHANGRONG HE and ZIHUI LAI

About the authors

Qun Chen *
Sichuan University,
College of Hydraulic and Hydropower Engineering,
State Key Laboratory of Hydraulics and Mountain River Engineering
Chengdu 610065, China
E-mail: chenqun@scu.edu.cn

Li Wan
Sichuan University,
College of Hydraulic and Hydropower Engineering,
State Key Laboratory of Hydraulics and Mountain River Engineering
Chengdu 610065, China
E-mail: wanali0266@tom.com

Changrong He
Sichuan University,
College of Hydraulic and Hydropower Engineering,
State Key Laboratory of Hydraulics and Mountain River Engineering
Chengdu 610065, China
E-mail: hechr@126.com

Zihui Lai
China Railway Eryuan Engineering Group Co. Ltd.,
Chengdu 610031, China
E-mail: TEYLJ1@creegc.com

* Corresponding author

Abstract

The piled retaining wall is a new type of railway retaining structure in China. In the current design, the retaining wall, the beam and the piles are assumed to be independent components. Both the mutual action of the retaining wall, the piles and beam, and the influence of the soil or rock foundation on the structure are not fully considered, so that there are some limitations in the current design method. In this paper, using field observations and a three-dimensional finite-element analysis, the lateral earth pressure on the wall back, the stress distributions and the forces of the reinforcements in the beam and the pile were studied. The simulation results were in good agreement with the field observation data. These results revealed that the tensile stresses were very small and that these stresses were positive in most zones in the beam and the pile. It can also be observed that the tensile stresses or forces in the beam and pile obtained in this study were much smaller than those obtained using the current design method. This clarified the fact that the current design method used for the beam and the pile was very conservative and that it should be optimized to consider the effect of the foundation on the whole structure and the interactions among the different components.

Keywords

piled gravity retaining wall, field observation, finite-element analysis, stress, load transfer mechanism

1 INTRODUCTION

Assuming that the bearing capacity of the foundation is insufficient, the pile foundation can be used to reduce the impact of the construction of a new railway on the already-existing railway and to guarantee the stability of the foundation. For this reason the piled retaining wall has been widely used in railway sub-grade engineering in recent years in China. However, a simple structural mechanics method is used in the design of the retaining structures. The retaining wall, the beam and the piles are considered as independent components, and both the mutual effect of the retaining wall, the piles and the beam, and the influence of the soil or rock foundation on the structure are not fully considered in the current design method, which is not in accordance with the facts. With the widespread use of this new type of retaining structure, it is necessary to systematically study the stress, deformation and load-transfer mechanism of all the components of the piled retaining wall to provide a theoretical basis for the design.

Usually, the piled retaining wall is composed of a retaining wall, a capping beam and some piles. The capping beam is a load-transfer component between the wall and the piles. This structure can be divided into two types: the piled gravity and the piled weighing retaining wall, according to the type of retaining wall. The former is the

common gravity wall, while the latter has a weighing platform at the back of the wall. Generally, the retaining wall is made of concrete, and the beam and the pile are made of reinforced concrete (RC).

The piled retaining wall has not been reported in countries other than China. In recent years, some researchers in China have studied the load transfer and the design method of the piled retaining wall. The mechanical characteristics and load-transfer mechanism of the piled weighing retaining wall were studied using a numerical method [1]. The mechanical principle of the piled weighing retaining wall was also investigated through a physical model test [2]. A modified design method for the piled retaining wall was proposed, based on research on a load applied to the structure [3].

The research results mentioned above have touched upon the interaction among the piles, the beam and the retaining wall, and the load-transfer mechanism of the structure. They also introduced some simplified calculation methods, which can be used for the design as references. However, most of them just focused on the piled weighing retaining wall. The mechanical characteristics of the piled gravity retaining wall were seldom reported. Moreover, so far, there is no report about a field study that can be used to verify the results obtained by a numerical simulation or a physical model test. In this paper, field observations and a three-dimensional finite element analysis were used to study the lateral earth pressure on the wall back, the stress distributions and the forces of the reinforcements in the beam and the pile. The results obtained in this work were also compared with those using the current design method. Some valuable advice is presented to support the design of piled retaining walls in the future.

2 PROJECT CONDITIONS AND INSTRUMENTATION

The piled gravity retaining wall studied in this paper is located at the station DK242+113 to DK242+155 on the double line railway, with a speed of 200 km/h, from Dazhou to Chengdu city in the Sichuan Province of China. The wall is 42 m long and its maximum height is 10 m. The surface layer of the foundation is silty clay, 1 m to 10 m thick, under which there are soft mudstones with a little sandstone. The ground surface is inclined and the foundation would not be stable if a common gravity retaining wall was used; therefore, a piled gravity retaining wall was used to ensure the stability of the foundation of the railway.

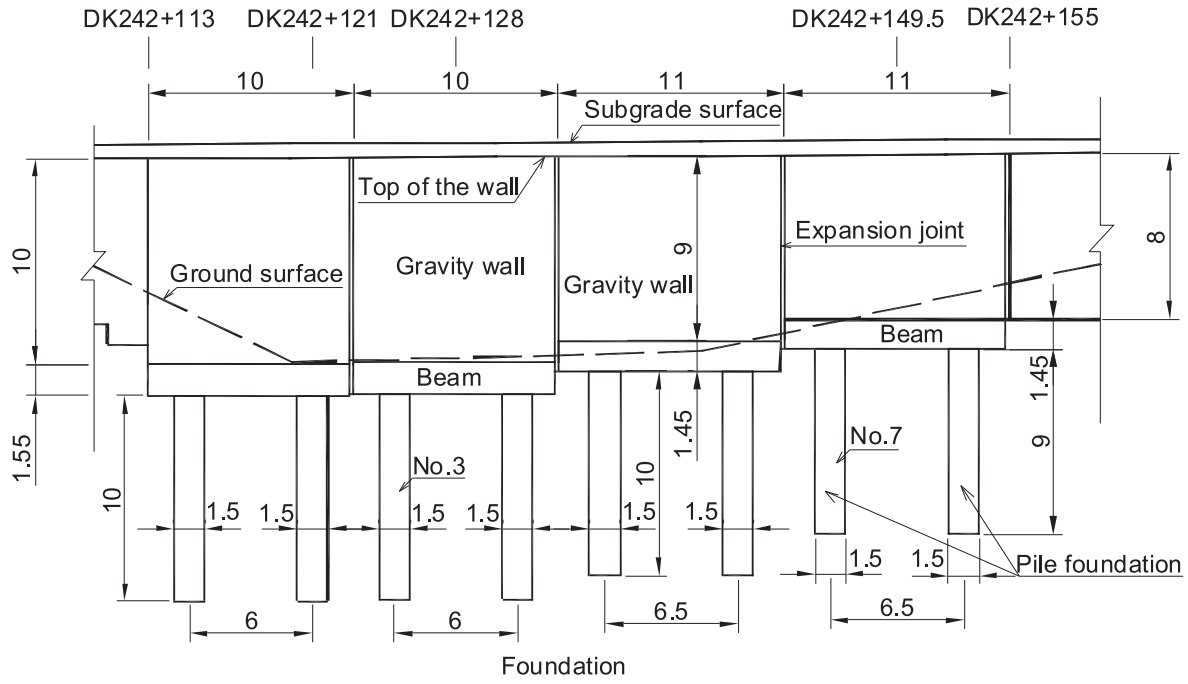

Figure 1. Front view of the piled gravity retaining wall (all units in meters).

The piled gravity retaining wall consists of four wall segments. They are two segments that are 10 m high and 10 m long, one segment that is 9 m high and 11 m long, and one segment that is 8 m high and 11 m long. The dimensions of the beam of the wall segment that is 10 m high are 10 m, 4.6 m and 1.55 m for length, width and thickness, respectively. Accordingly, they are 11 m, 4.0 m and 1.45 m for both wall segments that are 9 m and 8 m high. The dimensions of the piles of the 10 m and 9 m high wall segments are 10×2.25×1.5 m (length×width×thickness) and those of the 8 m high wall segment are 9×2.0×1.5 m. The front view and the cross-sectional geometry at the station DK242+121 of the wall are shown in Fig. 1 and Fig. 2, respectively. The backfill soil is compacted silty clay with some mudrock debris.

In order to study the stresses or forces on the structure, the lateral pressures on the back of the retaining wall and the stresses at the interface between the wall and the beam, two typical wall segments were chosen for the instrumentation. One is the wall segment that is 10 m high and the other is the wall segment that is 8 m high. The central cross-sections (station DK242+128 and station DK242+149.5 shown in Fig. 1) are chosen to install the earth pressure cells. The piles No. 3 and No. 7 (in Fig. 1) are chosen to install the reinforcement gauges. Due to space restrictions, only the results of the former wall segment (10 m high) will be presented and discussed.

Ten vibrating-wire earth pressure cells with a vertical spacing of 1 m were mounted on the wall back to measure the lateral earth pressure (shown in Fig. 3). The upmost earth pressure cell was located 0.5 m away from the top of the wall.

In order to monitor the stress distribution at the interface between the wall and the beam, ten rosettes of vibrating-wire strain gauges were installed at the interface. There were four strain gauges in each strain rosette to measure the strains along the directions of 0˚, 45˚, 90˚ and 135˚ at the same point. The strains in one half of the beam were measured because of their symmetrical distribution to the span center line in the beam. The arrangement and the orientation of the strain gauges in each strain rosette are shown in Fig. 4.

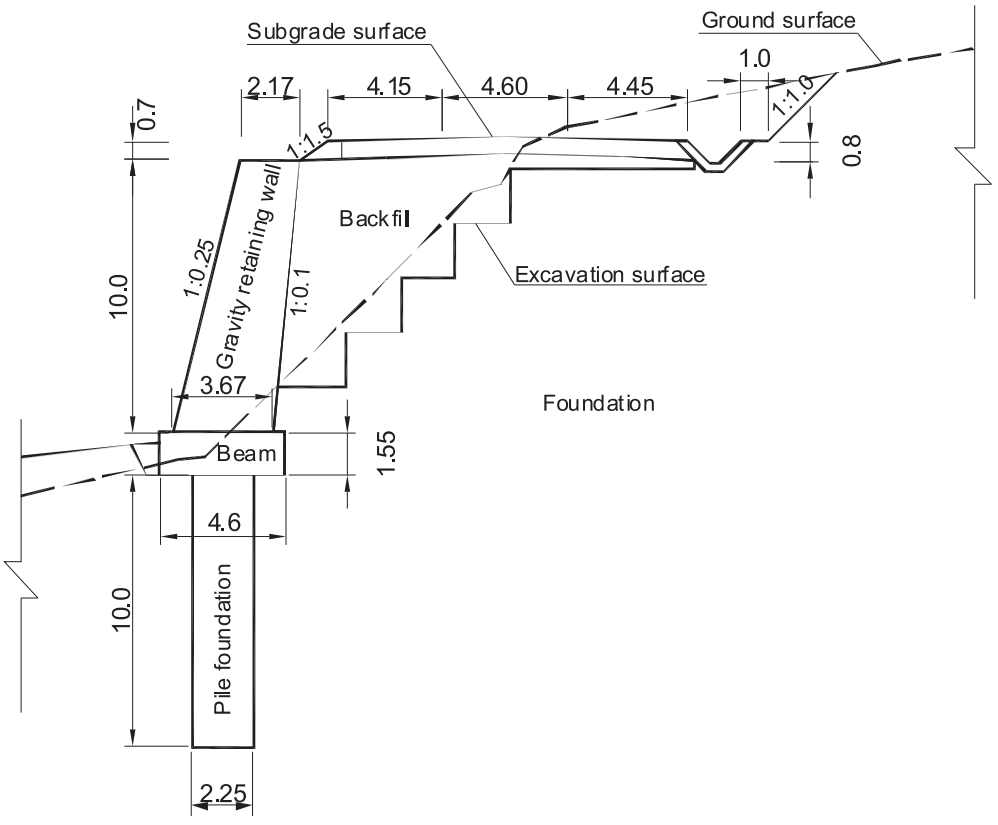

Figure 2. Cross-sectional geometry of the piled gravity retaining wall at station DK242+121 (all units in meters).

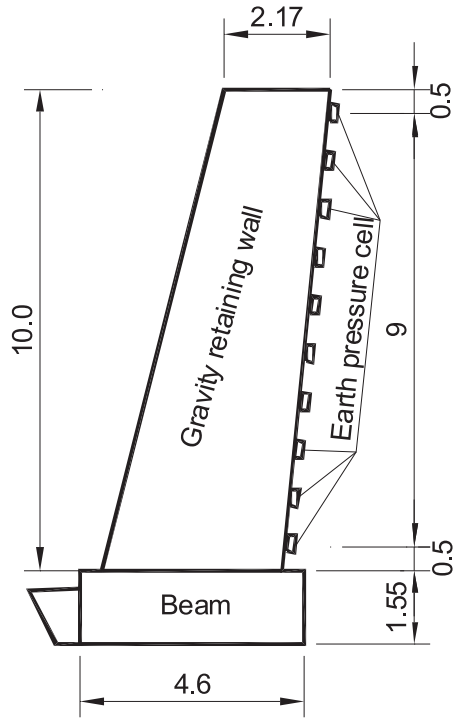

Figure 3. Arrangement of the earth pressure cells on the wall back (all units in meters).

The beam can be considered as a plane strain member, so that its longitudinal (x axis) strain can be ignored. When the strain direction of 0° aligns with that of the y axis, the normal strains in the four degree directions and the strain components in Cartesian coordinates have the following relations [4]:

$$\begin{aligned} &\varepsilon_y = \varepsilon_0 \\ &\varepsilon_z = \varepsilon_{90} \\ &\gamma_{yz} = \varepsilon_0 + \varepsilon_{90} - 2\varepsilon_{45} \quad or \quad \gamma_{yz} = 2\varepsilon_{135} - (\varepsilon_0 + \varepsilon_{90}) \end{aligned} \tag{1}$$

where ε_0, ε_{45}, ε_{90} and ε_{135} are the measured normal strains in four degree directions in one strain rosette, as shown in Fig. 4(b); ε_y and ε_z are the normal strains in the y and z directions respectively; and γ_{yz} is the shear strain in the z direction on the Y plane. According to the generalized Hooke's law [4], the horizontal and vertical normal stresses and the shear stress can be calculated by:

$$\begin{cases} \sigma_y = \dfrac{E[(1-\mu)\varepsilon_0 + \mu\varepsilon_{90}]}{(1+\mu)(1-2\mu)} \\ \sigma_z = \dfrac{E[(1-\mu)\varepsilon_{90} + \mu\varepsilon_0]}{(1+\mu)(1-2\mu)} \\ \tau_{yz} = \dfrac{E(\varepsilon_0 + \varepsilon_{90} - 2\varepsilon_{45})}{2(1+\mu)} \text{ or } \tau_{yz} = \dfrac{E(2\varepsilon_{135} - \varepsilon_0 - \varepsilon_{90})}{2(1+\mu)} \end{cases} \tag{2}$$

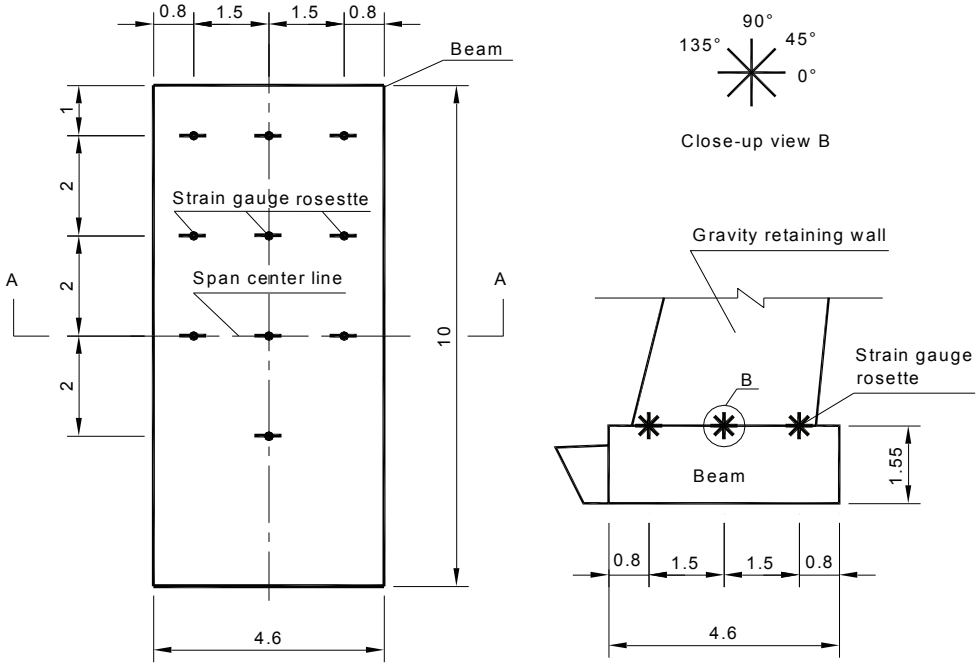

Figure 4. Arrangement of the strain gauges at the interface between the wall and the beam (all length units in meters).

where E and μ are the elastic modulus and the Poisson's ratio of the material, respectively; σ_y and σ_z are the normal stresses in the y and z directions respectively; and τ_{yz} is the shear stress in the z direction on the Y plane. For the commonly used 45° strain rosette, the 0°, 45° and 90° strains are required to deduce the normal stresses and the shear stress. The 135° strain gauge is normally used for the proof measurement.

In order to investigate the forces of the reinforcements in the beam and the pile, many reinforcement gauges were welded to the reinforcement at the selected location. On the top of the beam, fifteen reinforcement gauges were welded to three reinforcements. Five reinforcement gauges with a spacing of 1.1 m were arranged in each reinforcement bar. The quantity and the arrangement of the reinforcement gauges at the bottom were the same as that on the top of the beam, as shown in Fig 5(a). In total, sixteen reinforcement gauges were welded to two reinforcements in the vertical center section of the pile: half were at the front side and the other half were at the back side, as shown in Fig 5(b).

Prior to the in-situ installation, all the earth pressure cells, strain gauges and reinforcement gauges were calibrated indoors and their original readings were recorded. The pressure, strain and the force can be computed using the calibrating coefficient and the frequency reading.

3 THREE-DIMENSIONAL FINITE-ELEMENT ANALYSIS

The three-dimensional finite-element software ADINA 8.4 [5] was used in this study to simulate the construction of the piled gravity retaining wall. ADINA is popular finite-element software and has been under development for more than thirty years. The use of ADINA for soil-structure interaction problems was described by Sumino et al. [6] and Chen & Krauthammer [7]. The software has also been used for an analysis of the axial pile capacity [8] and the stress transfer between the pile and the soil [9].

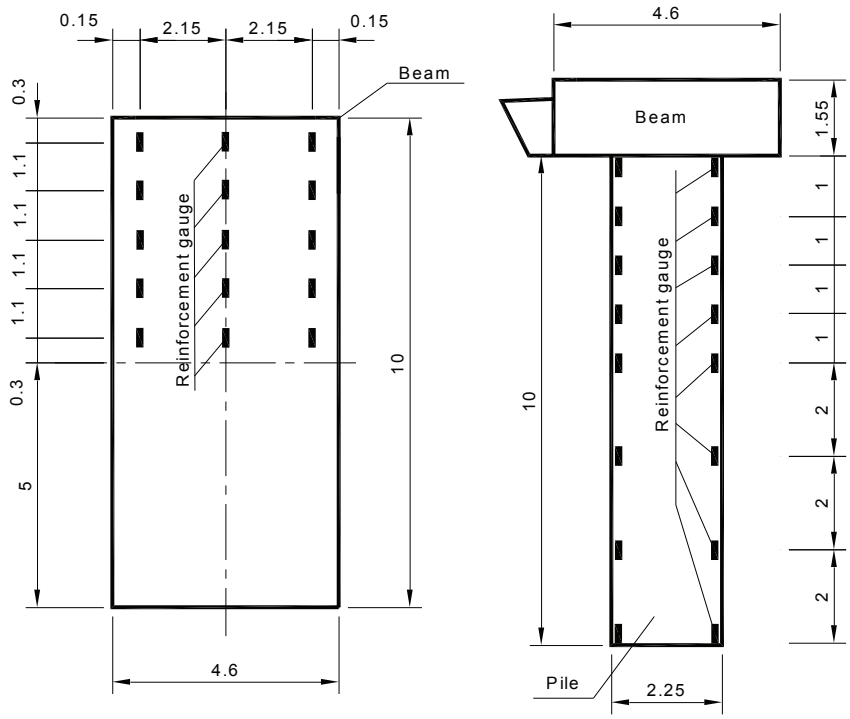

a) Horizontal section of the top or the bottom of the beam

b) Vertical center section of the pile

Figure 5. Arrangement of the reinforcement gauges on the top and at the bottom of the beam and the vertical center section of the pile (all units in meters).

To compare the results of the field observation, the wall segment that is 10 m high and 10 m long was analyzed in this paper.

3.1 SIMPLIFICATION AND DISCRETION OF THE FINITE-ELEMENT MODEL

The simulation domain was 10 m long (wall segment length), 46 m wide and 37.7 m high, as shown in Fig. 6. The origin of the coordinate was at the center, on the top of the beam. The longitudinal direction is defined as the *x* axis; the widthwise direction is defined as the *y* axis and the positive direction points to the wall; the altitudinal direction is defined as the *z* axis, and the upward is positive.

The concrete wall, the RC beam and piles, the backfill soil, the foundation soil and the rock were simulated using solid elements. Interface elements were assigned to the interface between the wall back and the soils. The thin layer elements were assigned between the wall and the beam because there was a construction interface.

The whole simulation domain was meshed to 62856 elements with 39241 nodes using 8-node hexahedron and 4-node tetrahedron elements. Smaller elements were used for the backfill soil. The surface mesh of the simulation domain is shown in Fig. 6. The mesh of the gravity retaining wall, the beam and the piles is shown in Fig. 7. The whole foundation was composed of two parts: the upper (above the bottom of the beam) and the lower parts. They were silty clay and mudrock, respectively.

The longitudinal end vertical boundaries were fixed to prevent movements to the boundaries' normal direction (fixed in the *x* direction). The left-hand and right-hand vertical boundaries were fixed in the *x* and *y* directions. The base was pinned, to prevent any movements in all directions (as shown in Fig. 6).

3.2 MATERIAL PROPERTIES

The backfill soil, foundation soil and mudrock were modeled using the Mohr-Coulomb elastic-plastic model which is capable of accounting for the dilation of soils.

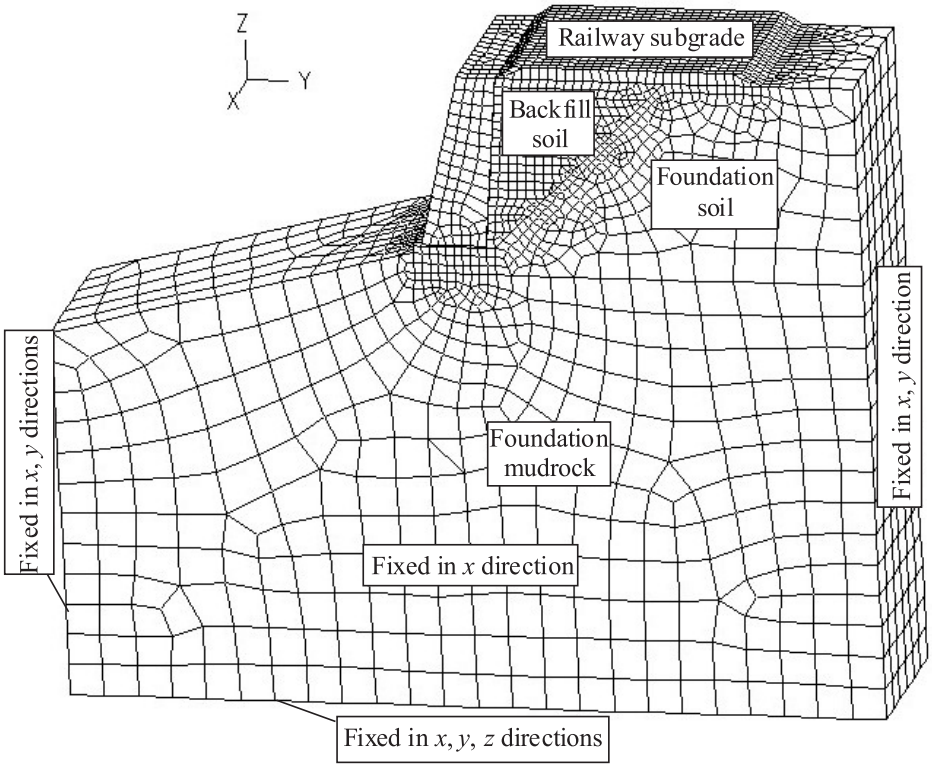

Figure 6. Surface mesh and boundary conditions of the simulation domain.

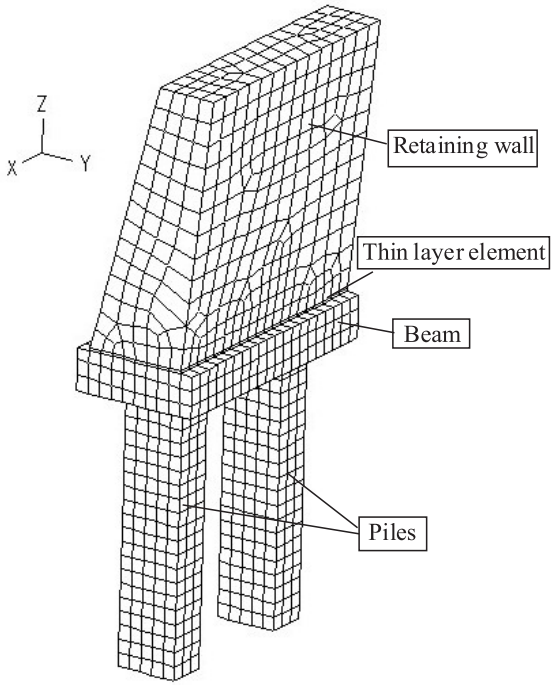

Figure 7. Surface meshes of the retaining wall, the beam and the piles.

The thin layer elements between the wall and the beam were also simulated using the Mohr-Coulomb model. Considering that the concrete wall and the RC beam and pile are much more rigid than the foundation and the backfill soil, all the structure components were assumed to be elastic material.

The property parameters of the RC and the concrete for the finite-element analysis were adopted according to the code GB50010-2002 [10]. The elastic constants of the thin layer element between the wall and the beam were the same as the concrete. Its strength parameters were referred to the shear strength parameters of the interface between the concrete layers in Table D3 in the design specification DL5108-1999 [11]. The constitutive model parameters of the soils and mudrock were obtained using a triaxial test. Their moduli and Poisson's ratios were obtained with a confined compression test and a uniaxial compression test. The frictional angle between the wall back and the soil was assumed to be half of the internal frictional angle of the backfill soil. All the material parameters used in the finite-element analysis are listed in Table 1.

3.3 MODELING OF THE CONSTRUCTION PROCEDURE

The construction procedure of the beam, the retaining wall and the embankment of the backfill soil were simulated using a finite-element analysis. The piles were considered as an already-existing structure for the foundation soil and rock because they were the bored cast-in-place piles and their construction had little impact on the stress and deformation of the foundation. Both the beam and the retaining wall were simulated as a single construction step. The filling of 1 m of backfill soil was modeled as a single placement step and the upper 0.7 m subgrade was modeled as a separate placement step.

As the groundwater table was lower than the base of the simulation domain and the backfill soil was compacted with lower water content than its optimal value, it was assumed that the pore-water pressures throughout the placement of the soil were zero at any stage. The initial vertical stresses in the backfill soil were computed by the gravity of the soil and the linear analysis. The horizontal stresses were calculated by the coefficient of the earth pressure at rest, which can be calculated using Poisson's ratio.

Table 1. Material parameters used in finite element analysis.

Parameters	Density	Modulus	Poisson's ratio	Cohesion	Internal friction angle	Dilation angle
Symbol	ρ	E	μ	c	φ	ψ
Unit	g/cm^3	MPa	-	kPa	°	°
Reinforcement concrete	2.4	3.1×10^4	0.2			
Concrete	2.3	2.2×10^4	0.2			
Thin layer element	2.3	2.2×10^4	0.2	500	26.6	0
Foundation mudrock	2.2	500	0.22	1200	24	10
Foundation soil	2.0	60	0.32	35	30	5
Backfill soil	1.9	40	0.35	35	28	3

4 RESULT ANALYSES AND DISCUSSION

The sign regulation of the ADINA is in accord with ordinary elastic mechanics. The tensile stress is positive and the compressive stress is negative. To facilitate the comparison of the numerical analysis results and the field observation data, the same coordinates were assigned to the field observation and analysis results.

4.1 PRESSURE ON THE WALL BACK

Fig. 8 shows the measured and computed pressures on the wall back. The pressures on the wall back increase with the progressive filling of the backfill soil and the pressure distributions along the height of the wall almost maintain the same mode during backfilling. The computed pressure distributions along the height of the wall are similar to the measured ones, although the pressure values obtained with the finite-element analysis are larger than the measured results. Both the measured and computed pressures increase gradually from upside to downside and decrease at the bottom of the wall back.

It is reasonable that the computed horizontal earth pressures are smaller than those of the dry-stone retaining wall obtained by Harkness et al. [12] because the cohesion of the backfill soil was considered in this analysis. The measured earth pressures are smaller than the computed ones; however, in the meanwhile, the measured stress changes at the base of the wall contributed by the placement of the backfill are a little larger than the computed ones. All of these indicate that the earth pressures are under-measured. The reason may be due to a system error of the pressure cells. It is also possible that the pressure cells are not closely contacted with the compacted backfill as the backfill near the wall back cannot be compacted by the machine effectively, the result of which is that it is relatively loose.

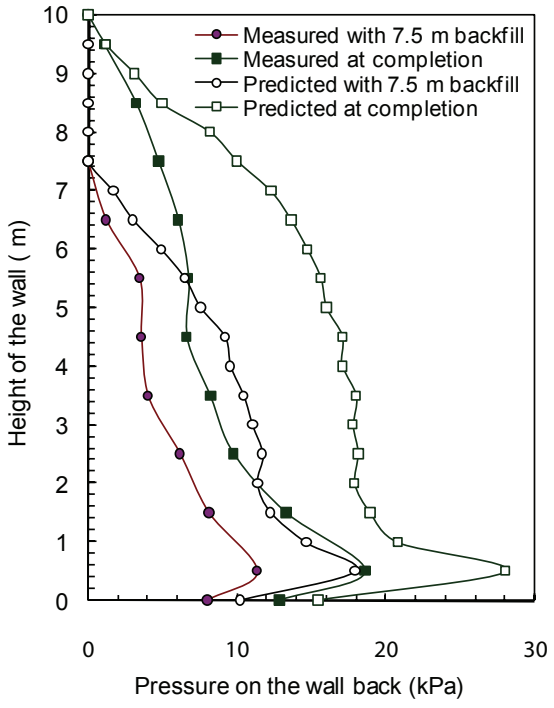

Figure 8. Measured and computed pressures on the wall back.

4.2 SHEAR STRESS BETWEEN THE WALL AND THE BEAM

The shear stress in the *y* direction at the interface between the wall and the beam can reflect the transfer of the lateral earth pressure on the wall back to the beam. The measured and computed shear stress distributions along the width direction of the beam at the interface between the wall and the beam at different construction stages are given in Fig. 9. A negative shear stress means the direction of the stress is towards the front of the wall. Both the measured and computed shear stresses are negative and they have similar distributions along the width direction of the beam, although the computed values are smaller than the measured ones. In different cross-sections, the shear-stress distributions represent a similar regulation. At the center of the width ($y = 0$), the magnitudes of the shear stresses are smaller than that at both sides of the beam. In the span center section ($x = 0$, Fig. 9(a)), the measured shear stresses and computed ones are a little larger at the front side than those at the back side. In the other sections (Fig. 9(b) and (c)), both the measured and computed shear stresses are smaller at the front side than those at the back side. They increase with the increasing height of the backfill soil. This is because the horizontal pressures on the back of the wall increase with the increase in the backfilling.

4.3 STRESSES OR FORCES IN THE BEAM

There is no strain gauge to measure the normal stress in the *x* direction in the beam, but the reinforcement gauge can measure the axial force of the reinforcement along the *x* direction. Fig. 10 illustrates the measured axial force distributions along the reinforcement and computed normal stress distributions in the *x* direction along the length direction on the top of the beam at different construction stages. Except for the computed

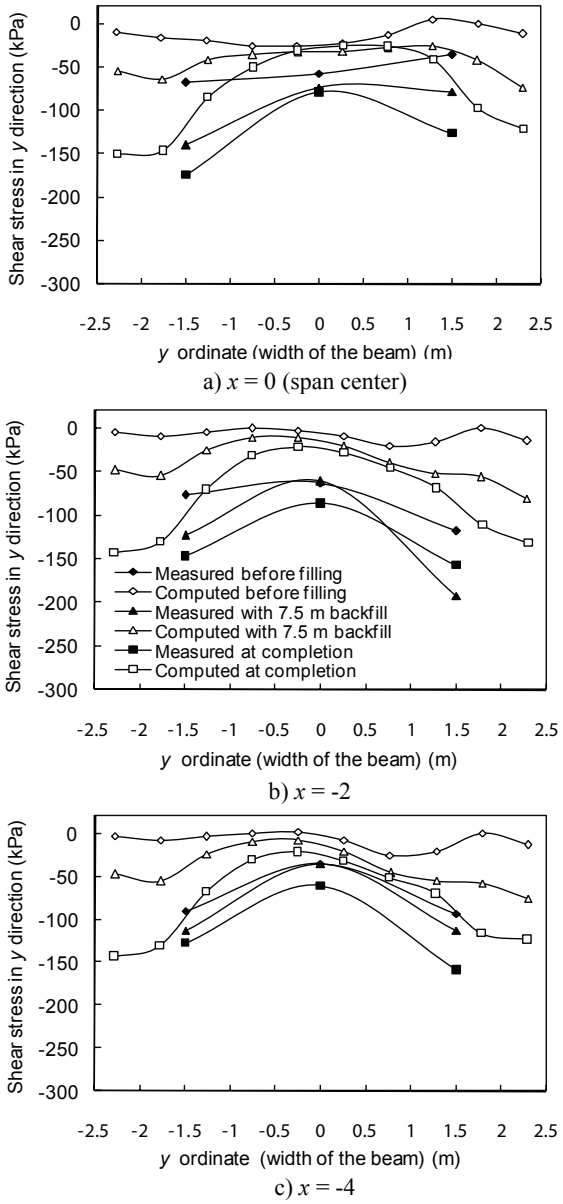

Figure 9. Measured and computed shear stresses in the *y* direction at the interface between the wall and the beam.

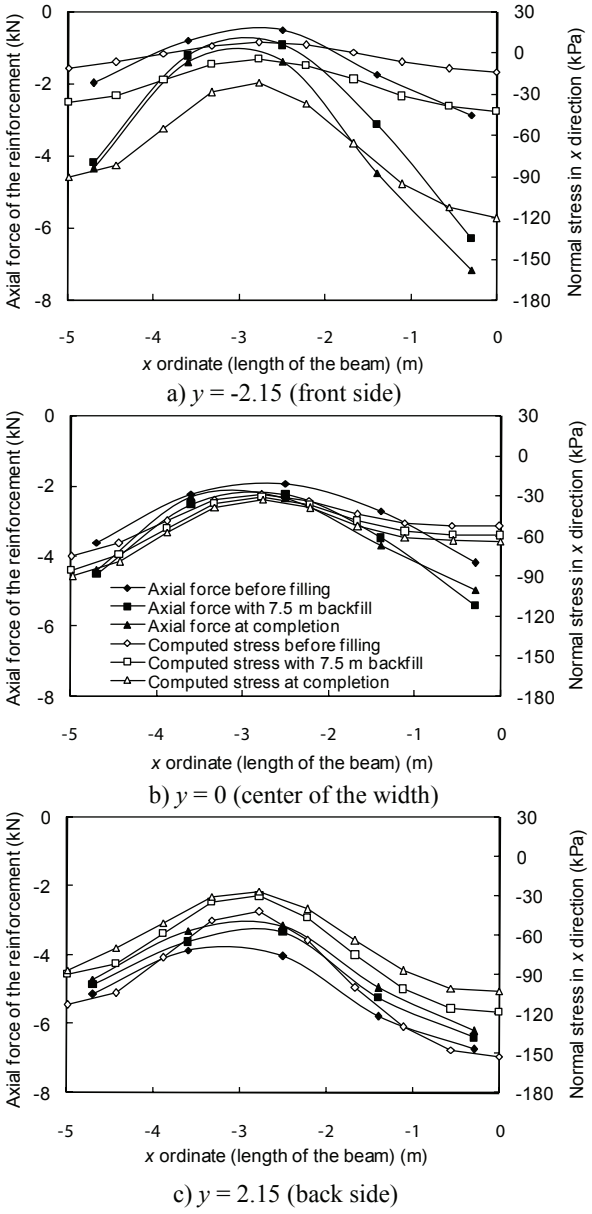

Figure 10. Measured axial forces of the reinforcements and computed normal stresses in the *x* direction on the top of the beam

stresses at the corresponding location of the pile top before filling, the forces and the stresses are both negative at different construction stages. This indicates that there is no tensile stress in the *x* direction as the top of the beam is compressed. Therefore, there is no need to use reinforcement for bearing the tensile forces. In the different longitudinal sections the stresses and the forces are similarly distributed along the length of the beam. They are the smallest at the corresponding location of the top center of the pile and become larger at the span center and the end of the beam, which is due to the underpinning effect of the pile on the beam. Although the underpinning effect results in tensile stresses in the beam, the top of the beam is still compressive due to the counter effect of the foundation mudrock, which weakens the moment effect.

Both the measured forces and the computed stresses increase with the increase in the height of the backfill soil at the front side and the center of the beam. However, they decrease with progressive backfilling at the back side of the beam. This is because the lateral earth pressure on

the wall back increases with the increase in the height of the backfill soil and makes the vertical compressive concentration zone, induced by the underpinning of the pile on the top of the beam, move from the back to the front side gradually with the construction process.

Fig. 11 shows the measured and computed normal stress distributions in the *y* direction along the width direction on the top of the beam at different stages of construction. The computed and measured stresses have similar distributions on the top of the beam, although the computed stresses are a little smaller than the measured ones at most locations. The stresses are negative in most zones and their distributions are similar in the different cross-sections. The stresses increase at the front and decrease at the back of the beam during the backfilling. Before placing the soil, the stresses are smaller in the front than those at the back. After filling the subgrade (at the completion), the stresses become larger in the front than those at the back. This is due to the increase in the lateral earth pressure, resulting in an increase of the normal stresses in the *y* direction in the beam.

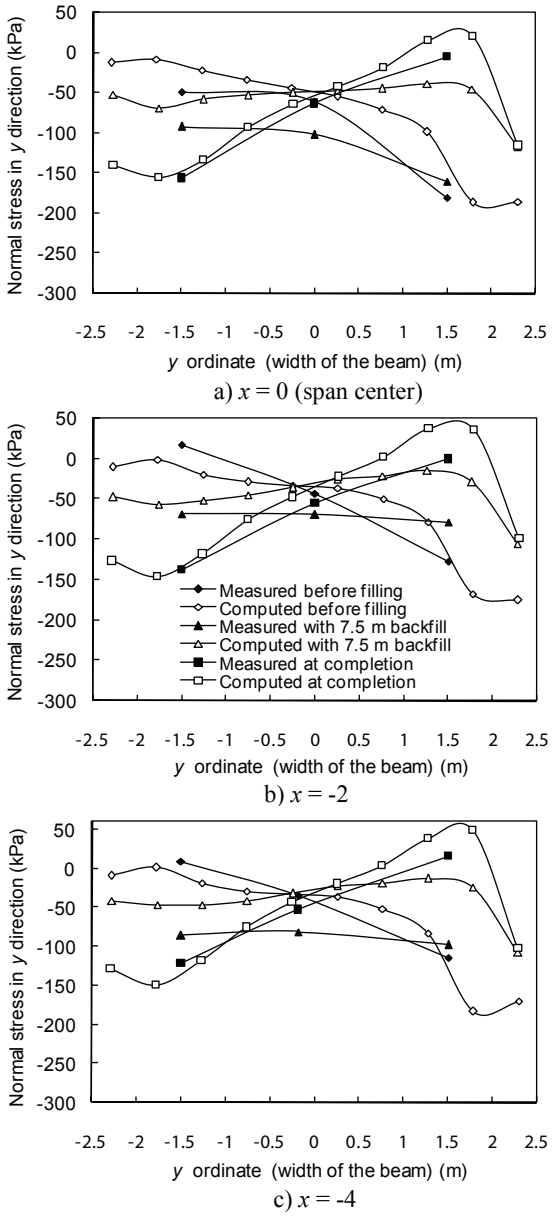

Figure 11. Measured and computed normal stresses in the *y* direction on the top of the beam.

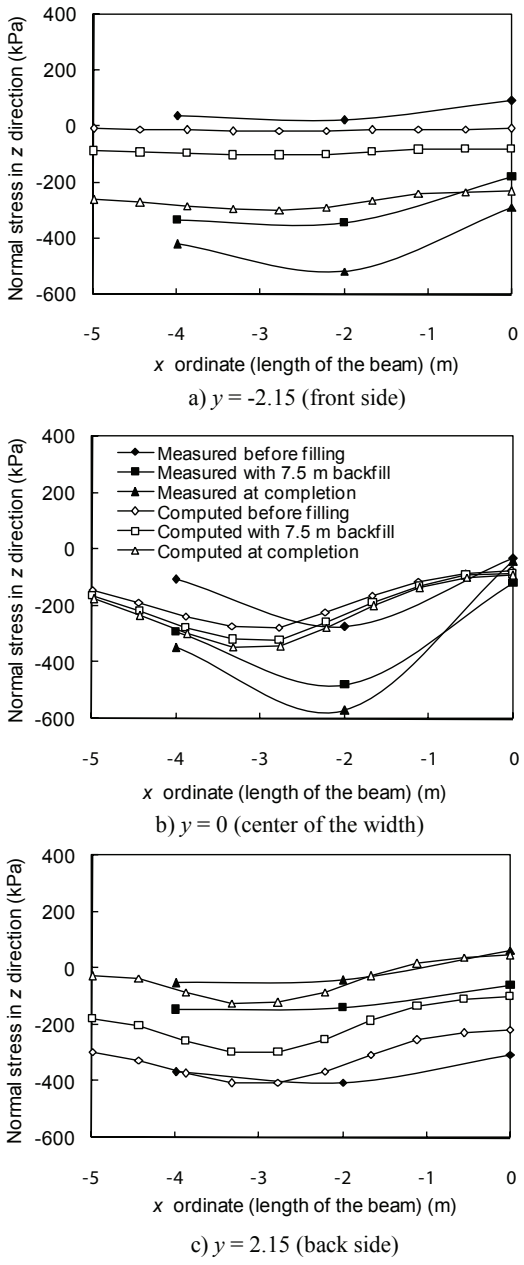

Figure 12. Measured and computed normal stresses in the *z* direction on the top of the beam.

The measured and computed normal stress distributions in the *z* direction along the length direction on the top of the beam at different construction stages are shown in Fig. 12. Although the computed and the measured stresses have a slight discrepancy, they show some common regulations. They are both negative in most zones and the beam is mostly compressed in the *z* direction. Except for the front side of the beam, the stresses are the maximum at the corresponding location of the top of the pile and then decrease to both sides. At the front side and the center of the beam (Fig. 12(a) and (b)), the stresses increase with the placement of the soil, while at the back side (Fig. 12(c)), the stresses decrease with the backfilling. This is because the increase in the lateral earth pressure with the backfilling makes the compressive concentration zone move from the back side to the front side on the top of the beam during backfilling.

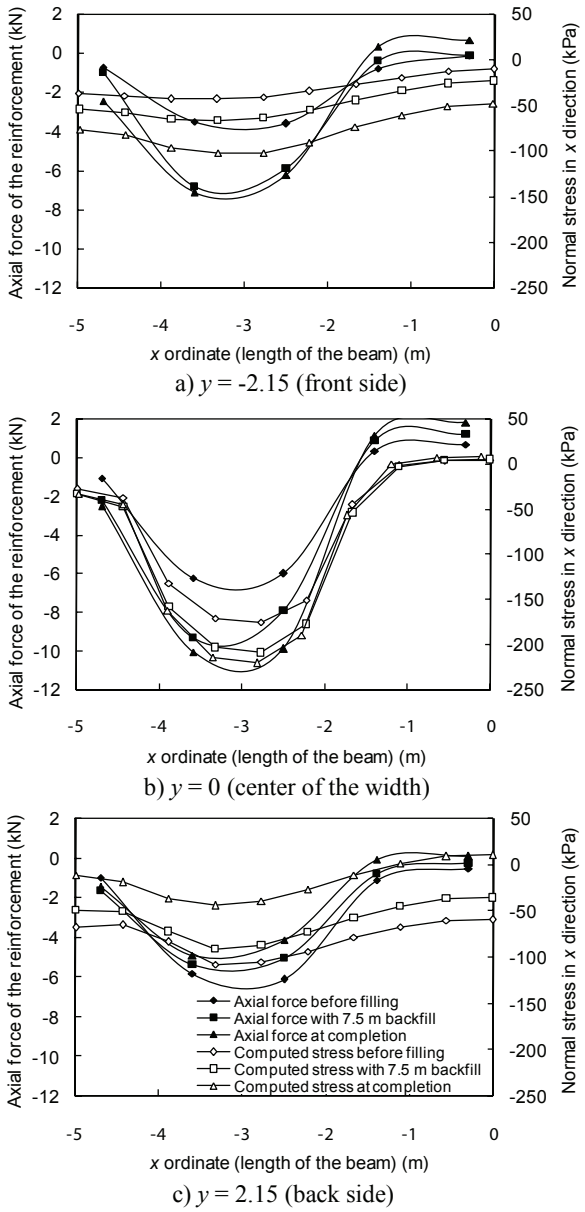

Figure 13. Measured axial forces of the reinforcements and the computed normal stresses in the *x* direction at the bottom of the beam.

Fig. 13 shows the measured axial force distributions along the reinforcements and the computed normal stress distributions in the *x* direction along the length direction at the bottom of the beam for different construction stages. Except for a small zone near the span center (x=0), the measured axial forces and the computed stresses are both negative in most zones. This indicates that most zones of the bottom of the beam are compressed. It is clear that because of the bearing effect of the foundation, the tensile stress caused by the moment at the span center is not large enough to counteract the compressive stress transferred from the top of the beam. The forces and the stresses have almost the same distribution regulations. They are the maximum at the corresponding location of the top center of the pile and decrease to both sides. At the front side and the center of the beam (Fig. 13(a) and (b)), the forces and stresses increase with the placement of the soil, while at the back side (Fig. 13(c)) they decrease with the backfilling.

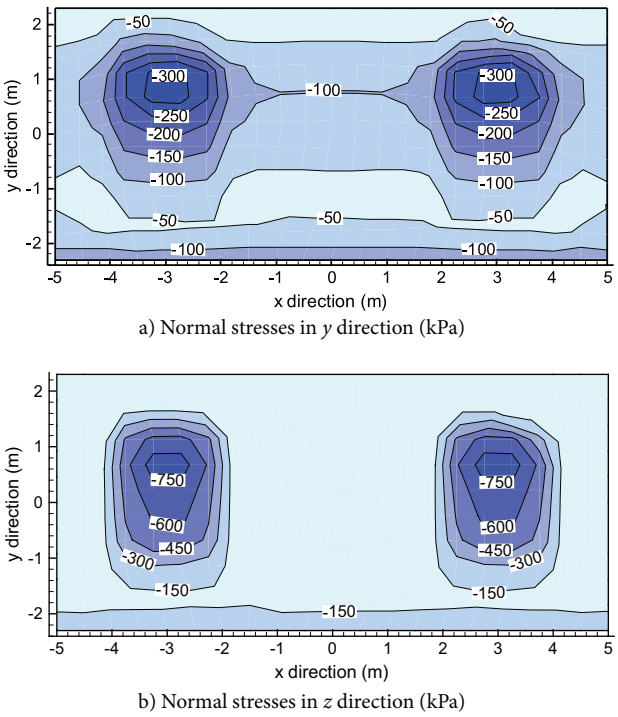

Figure 14. Contours of the normal stresses in the *y* and *z* directions at the bottom of the beam at the completion obtained with the finite-element analysis.

Due to there being no measured data available, the normal stresses in the *y* and *z* directions at the bottom of the beam are only represented by finite-element analysis results. Fig. 14 shows the contours of the normal stresses in the *y* and *z* directions at the completion. The stresses are all negative, which indicates that the bottom of the beam is compressed in both the *y* and *z* directions. There is a stress concentration zone at the location on the top of the pile, because the rigidity of the pile is higher than that of the mudrock foundation.

4.4 STRESSES OR FORCES IN THE PILE

The measured axial forces of the reinforcement and computed normal stresses in the *z* direction on the vertical center line at the front and the back sides of the pile are shown in Fig. 15. The forces and the stresses have similar distributions along the pile length. At the front side, the measured forces increase from the top to one-third of the pile length and decrease a little downwards to the end of the pile. The computed stresses increase from the top to the middle of the pile and then there is almost no change from the middle to the bottom. At the back side, the change of the forces along the pile length is small. The computed stresses have a small decrease from the top to the bottom of the pile. Because the weight of the backfill acts on the top of the beam and the foundation behind the wall, the back side of the beam has a settlement downwards; this results in an upward trend at the front side of the beam and tensile stress at the front side of the upper portion of the pile. Therefore, the compressive stresses or forces at the front side of the upper portion of the pile are smaller.

The horizontal load induced by the lateral earth pressure is transferred from the wall to the beam, and then to the top of the pile. The moment and the tensile stress will be induced in the pile if it is a member fixed at its bottom end and there is no restriction from the foundation. In contrast, the horizontal load is counteracted by the rock pressure on the side of the pile, because both sides of the pile are restricted by the foundation mudrock. So the pile is mainly compressed and has almost no tensile stress along its length.

With the placement of the backfill, both the measured forces and the computed stresses increase at the front side; nevertheless, the measured forces decrease at the

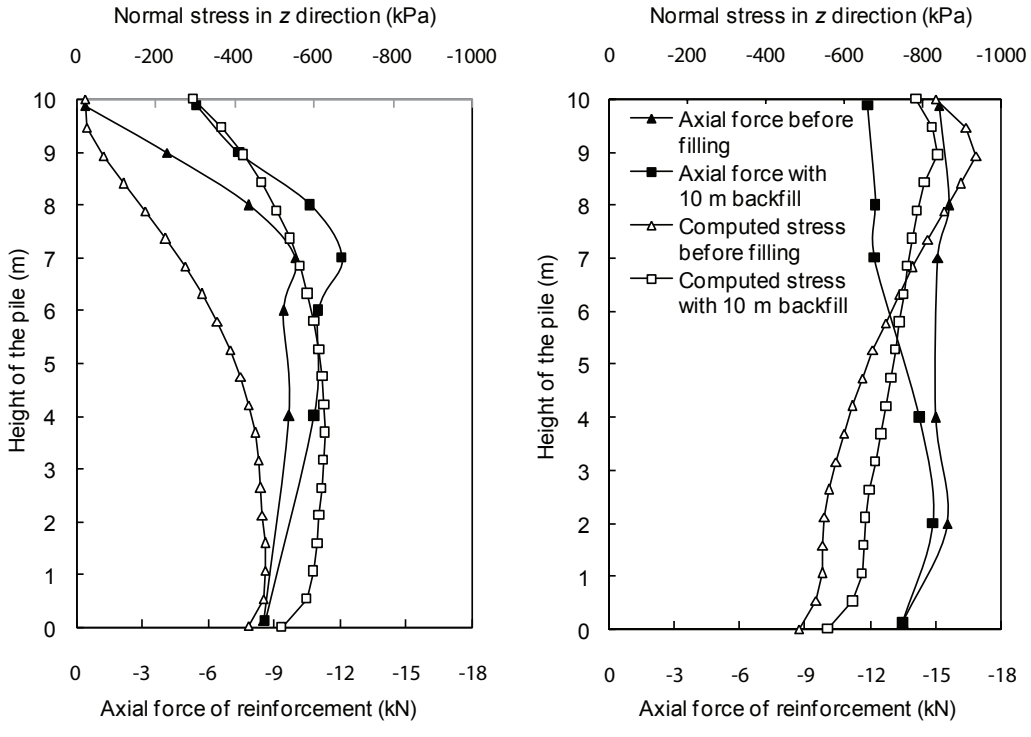

a) front side

b) back side

Figure 15. Measured axial forces of the reinforcements and computed normal stresses in the *z* direction along the vertical center line of the front and back sides of the pile.

back side, and the computed forces decrease in the upper 3.2 m of the pile length and increase in the lower portion. This illustrates that the back side of the pile is unloaded and the front side of the pile is loaded because the increase of the lateral earth pressure with backfilling makes the pressure concentration zone on the top of the beam move from the back to the front side.

5 COMPARISON WITH THE DESIGN RESULTS

For the design of the beam and the pile of the piled retaining wall, the tensile stress is the control factor for the quantity of reinforcement. In the current design method, the structural and material mechanics method is used to calculate the internal forces and stresses in the beam and the pile. A beam with two piles is considered as a frame-beam structure and the piles are assumed to be elastic foundation beams. The restriction of the rock foundation is simplified as the spring and the effect of the soil foundation are ignored. The load acting on the beam is from the weight of the wall and the lateral earth pressure, which together with the weight of the beam is considered as the loads acting on the top of the pile. Therefore, the wall, the beam and the pile are considered as individual components to calculate their internal forces and stresses.

The total lateral earth pressure on the wall back, the maximum tensile stresses in the beam and the pile in the directions of their length obtained by design calculation (according to the design report [13]) and finite-element analysis are listed in Table 2. The total lateral earth pressure on the wall back obtained by the design calculation is larger than that obtained by the finite-element analysis. This is mainly because the cohesion of the soil is not considered in the design calculation for safety. The maximum tensile stresses in the beam and the pile obtained by the finite-element analysis are much smaller than those obtained by the design calculation. Ignoring the interaction among the structure components causes the stresses in the beam and the pile to be overestimated in the design. In fact, there is little tensile stress in the beam and the pile, so the reinforcements do not take effect of bearing tensile forces. The reinforcement quantity is too much according to the tensile stresses obtained by the design calculation. This indicates the current design method is too conservative and should be updated.

6 CONCLUSION

Field observations and the three-dimensional finite-element method are used to study the stresses or forces and the load-transfer mechanism during the construction of the piled retaining wall. The simultaneous representation and comparison of the measured and finite-element-computed results verify that the three-dimensional finite-element method can acurately estimate the stresses of the beam and the pile. The results obtained by the finite-element analysis are in good agreement with the measured results.

The pressures on the wall back increase with the filling of the backfill soil and the pressure distributions along the height of the wall almost maintain the same mode during backfilling. The lateral earth pressures obtained by the design calculation are larger than that obtained by a finite-element analysis and field measurement.

The shear stresses in the *y* direction at the interface between the wall and the beam are towards the front of the wall, which indicates in the horizontal earth pressure being transferred from the wall back to the beam. Along the length of the beam, the shear stresses are smaller in the center and larger at both sides along the width of the beam. The normal stresses in the three directions on the top of the beam are all compressive in most zones and the tensile stresses only represent in a small range and their magnitude is very small. Because of the underpinning of the pile, the normal stresses in the *x* direction on the top of the beam are smaller and the normal stresses in the *z* direction are larger at the corresponding location of the top of the pile. During the placement of

Table 2. Comparison of finite-element analysis and design-calculation results.

Obtained method	Total lateral earth pressure (kN/m)	Maximum tensile stress on the top of the beam (kPa)	Maximum tensile stress at the bottom of the beam (kPa)	Maximum tensile stress in the pile (kPa)
Finite element analysis	207.52	73.13	11.83	None
Design calculation	273.00	1180.29	602.63	1829.14

the soil, except for a small area near the span center, the normal stresses in three directions at the bottom of the beam are all compressive.

The horizontal load transferring from the beam to the pile was counteracted by rock pressure on the front side of the pile. Thus the pile is mainly compressed and has almost no tensile stress along its length.

The comparison of the results of the finite-element analysis and the design calculation shows that the design calculation overestimates the tensile stresses in the beam and the pile, which causes a large waste of the reinforcement. According to the field observation and the finite-element analysis results, there are small tensile stresses in the beam and the pile. Therefore, the current design method should be revised so as to consider the interaction among all the structure components and consider the foundation effect on the structure reasonably.

ACKNOWLEDGMENTS

This research is substantially supported by a grant from the National Science Youth Foundation of China (Approved No. 50709022) and by the Support Program for New Century Excellent Talent in China (Approved No. NCET-07-0569). The authors would also like to thank Mr. He Guomin for his assistance with the field instrumentation.

REFERENCES

[1] Qiao, C. L. (2004). Study on Action Mechanism of Piled Retaining Wall, Master Thesis, Sichuan University, Chengdu, China. (in Chinese).

[2] Gao, Z. H. (2005). Experimental Study and Numerical Analysis of Mechanical Behavior of Piled Retaining Wall Structure, Master Thesis, Sichuan University, Chengdu, China. (in Chinese).

[3] Zhang, M. (2007). Study on Designing Theory and Engineering Application of Piled Retaining Wall Structure, Master Thesis, Xinan Jiaotong University, Chengdu, China. (in Chinese).

[4] Muvdi, B. B., McNabb, J. W. (1980). Engineering Mechanics of Materials, Macmillan Publishing Co., New York, USA.

[5] ADINA R&D, Inc. (2006). ADINA User Interface Command Reference Manual Volume I: ADINA Solids & Structures Model Definition, Watertown, MA 02472, USA.

[6] Sumino, K., Noguchi, H., Hyodo, K., Sekimoto, H. (1985). Application of ADINA in analysis of a soil structure, Comput. Struct., Vol. 21 (1-2), 51-61.

[7] Chen, Y., Krauthammer, T. (1989). Combined ADINA-finite difference approach with substructuring for solving seismically induced nonlinear soil-structure interaction problems, Comput. Struct., Vol. 32 (3-4), 779-785.

[8] Lai, P., McVay, M., Bloomquist, D., Badri, D. (2008). Axial pile capacity of large diameter cylinder piles, From Research to Practice in Geotechnical Engineering, GSP 180, ASCE, 366-383.

[9] Nie, R-S., Leng, W-M., Yang, Q., Wei, W. (2009). Discussion on shear stress transfer between pile and soil, Rock and Soil Mechanics, Vol. 30 (3), 799-804. (in Chinese).

[10] The Construction Ministry of People's Republic of China. (2002). GB50010-2002 Code for Design of Concrete Structures, China Architecture and Building Press, China. (in Chinese).

[11] The China East Survey and Design Institute of State Electric Power Company. (1999). DL5108-1999 Design Specification for Concrete Gravity Dams, China Electric Power Press, China. (in Chinese).

[12] Harkness, R. M., Powrie, W., Zhang, X., Brady, K. C., O'Reilly, M. P. (2000). Numerical modelling of full-scale tests on drystone masonry retaining walls, Geotechnique, Vol. 50 (2), 165–179.

[13] China Railway Eryuan Engineering Group Co. Ltd. (2007). Design Report of the Double Line Railway with a Speed of 200 km/h from Dazhou to Chengdu City. (in Chinese).